JOURNAL OF SOLID STATE CHEMISTRY 104, 412–421 (1993)

The Structural Features of Cobalt Oxides: ^{57}Fe Mössbauer Spectroscopy, TEM, and Static Magnetic Susceptibility Measurements

V. I. KUZNETSOV, V. A. SADYKOV,* V. A. RAZDOBAROV, AND A. G. KLIMENKO

Institute of Catalysis, Siberian Division of the Russian Academy of Sciences, pr.Lavrentieva 5, 630090 Novosibirsk, Russia

Received December 16, 1991; in revised form July 17, 1992; accepted October 15, 1992

^{57}Fe Mössbauer spectroscopy data obtained between 4.2 and 298 K, TEM, and magnetic measurements were used to study details of the real structure of cobalt oxides, CoO and Co_3O_4. In Co_3O_4 samples synthesized at low temperatures the tracer is nonuniformly distributed. It exists in the form of α-Fe_2O_3 inclusions generating stacking faults as well as in the form of Fe^{3+} ions in octahedral positions of the spinel matrix. An excess of oxygen in Co_3O_4 was found to generate cation vacancies in the octahedra. The two-phase CoO–Co_3O_4 system displays a dislocation network broadening the resonance lines and increasing the quadrupole splitting. For monophasic CoO an excess of oxygen leads to the formation of microclusters of Co_3O_4. A periodic array of shear type extended defects found in modified CoO was proposed to be generated by ordering of Fe impurities in some planes of the cubic structure.

Introduction

Physical and chemical properties of cobalt oxides are known to be strongly dependent upon their nonstoichiometry and real structure (*1–3*). However, accessible data are contradictory. According to Kotousova and Polyakov (*4*) and Angelov *et al.* (*5*), an excess of oxygen in Co_3O_4 generates vacancies in tetrahedral sites, which order in some planes. On the other hand, according to Belova *et al.* (*2, 6*), cation vacancies are situated in octahedra. Using ESR and magnetic measurements, Angelov *et al.* (*7*) have proposed the following model: all excesses of oxygen, as well as Co^{3+} ions in high-spin configuration, are localized in a subsurface layer, while the bulk of particles has a strictly stoichiometric composition. For CoO_{1+x} having small deviations from stoichiometry the dominant types of defects were thought to be cation vacancies in the octahedra (*1*). However, recent experimental results and model calculations enabled one to assume that clustering occurs at all but the very smallest deviation from stoichiometry (*8*). The surface of CoO was demonstrated to be enriched by oxygen to resemble that of Co_3O_4 (*9*). Pressing (i.e., plastic deformation) of CoO broadens Mössbauer resonance lines, probably due to generation of extended defects (*10*). Such uncertainty of conclusions about predominant types of defects in cobalt oxides made us to reinvestigate this problem. We have mainly used Mössbauer spectroscopy of ^{57}Fe tracer introduced in small quantities to minimize its influence on the defect structure of the materials under investigation. To date this method has been applied primarily to study the charge state of iron and its distribution between the cation sublattices (*10–14*), finer details of the defect structure practically not being taken into account. For a more reli-

* To whom correspondence should be addressed.

0022-4596/93 $5.00

TABLE I

THE CONDITIONS OF SAMPLE PREPARATION

Sample number	Temperature of calcination, gas phase, dynamic of cooling	Time of calcination, hr	Phase composition
1	673 K, air, slow cooling to room temperature	4	Co_3O_4
2	1073 K, air, slow cooling to room temperature	2	Co_3O_4
3	1273 K, air, air quenching	2	Co_3O_4, CoO
4	Sample 3 annealed in air at 1073 K, slow cooling to room temperature	4	Co_3O_4
5	1273 K, He (O_2 admixture <5 ppm), rapid cooling to room temperature in He	4	CoO

able interpretation of the Mössbauer spectroscopy data, the complementary methods such as transmission electron microscopy (TEM) and magnetic susceptibility measurements were employed.

Experimental

The samples were prepared as follows: a calculated amount of ^{57}Fe (99.999% purity, 97% enrichment) was dissolved in diluted (1 : 3) HNO_3 of "pure for analysis" grade and added into a solution of $Co(NO_3)_2$ of the same grade. After slow evaporation of this solution at ca. 373 K the dry residue was calcined in a muffle furnace at 673 K for 4 hr. Some more details of the sample preparation are given in Table I. According to Angelov *et al.* (*5, 7*), Co_3O_4 annealed at 673 K contains a considerable excess of oxygen, while calcined at 1073 K it is practically stoichiometric. Air calcination at 1273 K (sample 3) leads to the phase transition into CoO. An air quenching of this sample is accompanied by formation of a two-phase Co_3O_4–CoO system due to a partial reoxidation of CoO at temperatures lower than the phase transition temperature (1150 K) (*15*). The subsequent air annealing at 1073 K (sample 4) was performed to monitor the defect structure relaxation. Single-phase CoO (sample 5) was obtained by calcination of sample 4 in the T–p_{O_2} region where this phase exists (*15*), namely, at 1273 K in a flow of He (an admixture of O_2 is less than 5 ppm). However, by contact with air even at room temperature the surface layer of CoO particles could be oxidized up to a Co_3O_4 composition.

Mössbauer spectra were acquired using an NF-640 spectrometer in the temperature range 298–4.2 K. In all experiments, the source was ^{57}Co(Pd) at room temperature and calibration was via an enriched iron metal foil absorber. All spectra were fitted by the least-squares method to multiple Lorentzian peaks. Isomer shifts δ have been transformed to metallic iron at room temperature. Recoilless fractions f' were determined using the nonresonance filter method (*16*).

The real structure investigation was carried out by the use of a JEM-100CX electron microscope operating at 100 kV with ca. 3 Å resolution. The phase composition of the samples was determined by means of selected area electron diffraction.

The magnetic properties of the samples in weak magnetic fields were investigated using a SQUID magnetometer. The samples were placed in 5-mm-long quartz ampoules ca. 2 mm in diameter. The long axis of the sample was oriented along the magnetic field direction. Temperature dependence measurements of static magnetic susceptibility were carried out as follows. The sample was

cooled in zero magnetic field down to ca. 2 K, then the magnetic field was switched on and the full magnetic moment of the sample was measured as a function of temperature. The results were continuously recorded on a two-scale plotter.

Results

1. Electron Microscopy

Typical images of the samples under investigation are given on Fig. 1a–e. We have not observed any particles which could be attributed to admixture of an α-Fe_2O_3 phase.

Sample 1 (Fig. 1a) consists of aggregates of thin well-crystallized Co_3O_4 platelets. The observed faceting of the particles seems to be caused by stacking faults lying parallel to the image plane.

For sample 2 (Fig. 1b) calcined at 1073 K a change of particle morphology is observed. In this case particles have the form of square pyramids as evidenced by the typical extinction contours on their images. Probably, the formation of such particles goes via sintering of thin platelets by the most developed faces.

The particles of sample 3 (Fig. 1c) have the form of thick agglomerates. Their edges are characterized by a fairly developed dislocation network. The subsequent calcination at 1073 K causes its partial annealing (sample 4, Fig. 1d).

The calcination in He at 1273 K, despite the phase transition, preserves the morphology of the particles, with a periodical set of extended defects of a shear type appearing (Fig. 1e).

2. Mössbauer Spectroscopy

Mössbauer spectra of the samples measured at 298, 77, and 4.2 K are demonstrated in Figs. 2 and 3, while corresponding Mössbauer parameters are given in Table II. Both quadrupole splittings Δ directly observed in doublets and quadrupole shifts (splittings) ε obtained from sextet spectra by using relation the $\varepsilon = (\Delta_{56} - \Delta_{12})/4$ (Δ_{12} and Δ_{56}—splitting between lines 1–2 and 5–6 of the spectrum) are included in this table. The quadrupole shift is related to the quadrupole splitting by $2\varepsilon = \Delta\,(3\cos^2\theta - 1)/2$, with θ the angle between the electric field gradient (EFG) principal axis and the direction of the magnetic field.[1]

For sample 1 at 298 and 77 K a superposition of Zeeman sextet (M) and paramagnetic doublet (D) is observed, while at 4.2 K there is a superposition of two sextets (M_0 and M_1). Sextet M_0 corresponds to an α-Fe_2O_3 phase which remains in a weakly ferromagnetic state down to 4.2 K (no Morin transition is observed, ε being negative[1] (*17*)). According to Yamamoto (*12*) and Kündig *et al.* (*17*), such behavior of this phase indicates small (ca. 100 Å) typical dimensions of its particles. However, TEM does not reveal such particles of α-Fe_2O_3. Therefore, one may suppose that the Mössbauer spectroscopy data imply the presence of the α-Fe_2O_3 microinclusions within the Co_3O_4 particles.

For sample 2 at 298 and 77 K the superposition of a symmetrical paramagnetic doublet and six line magnetic hyperfine pattern corresponding to α-Fe_2O_3 was found. At 4.2 K two sextets, M_0 and M_1, were detected. According to Murray and Linnett (*13*) and Tricher *et al.* (*14*), the parameters of the doublet D for the samples 1 and 2 (Co_3O_4 phase) correspond to Fe^{3+} ions in Co_3O_4 matrix (i.e., spinel solid solution $Co_xFe_{3-x}O_4$). The transformation of doublet into sextet at 4.2 K can be explained by the transition of Co_3O_4 from a paramagnetic into a magnetically ordered antiferromagnetic state at ca. 40 K.

Sample 3 gives spectra consisting of the asymmetric doublet at 298 K and the superposition of symmetrical doublet and M_2 sextet at 77 K. According to Okand and Mullen (*10*), the M_2 sextet may be attributed to Fe^{3+} ions substituting for Co^{2+} ions in the cubic

[1] In the paper of Kündig *et al.* (*17*) a kind of quadrupole shift was defined by $\Delta_{12} - \Delta_{56}$ being positive for the weakly ferromagnetic state of hematite.

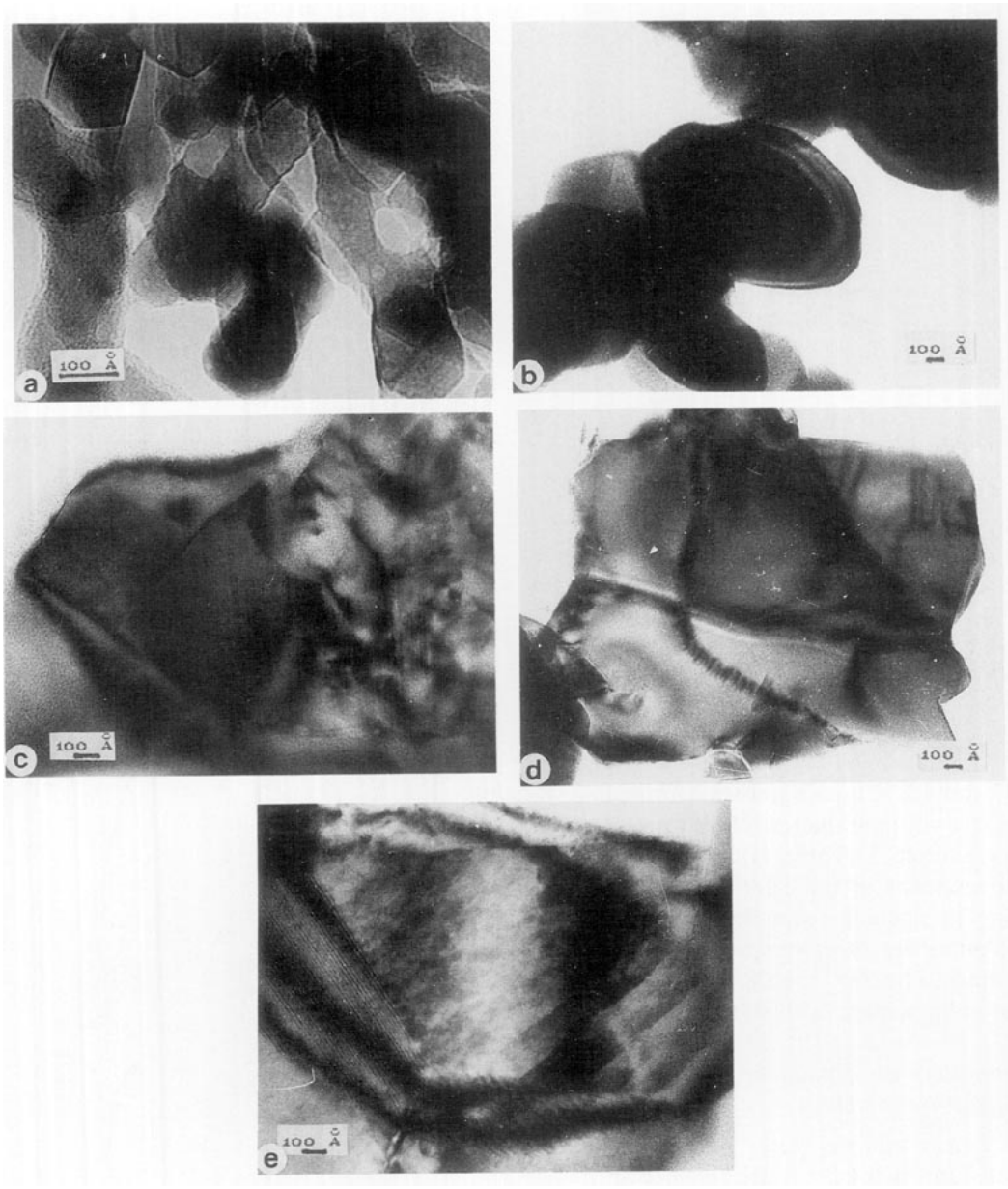

FIG. 1. Typical images of particles of cobalt oxides promoted by iron: (a) sample 1; (b) sample 2; (c) sample 3; (d) sample 4; (e) sample 5.

lattice of CoO. The Néel magnetic phase transition temperature, T_N, of the latter equals to 270 K.

For sample 4 only a symmetrical doublet was registered both at 298 and at 77 K, while at 4.2 K a Zeeman sextet (M_1) corresponding to Fe^{3+} ions in the Co_3O_4 spinel matrix appeared. The absence of M_2 sextet for sample 4 obtained from sample 3 by a long annealing at 1073 K is easily explained by the disappearance of CoO phase.

For sample 5 at 298 K the spectrum is the superposition of a singlet (Fe^{3+} in CoO) and a paramagnetic doublet (Fe^{3+} in Co_3O_4). At

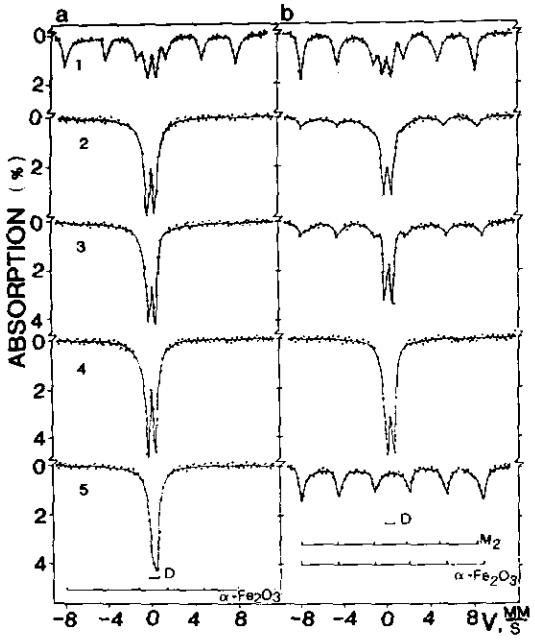

FIG. 2. Mössbauer spectra of the samples at 298 K (a) and 78 K (b). The curve numbers correspond to the samples numbers in Tables I and II.

77 and 4.2 K the singlet transforms into the sextet with parameters close to those of M_2 for sample 3 (Table II). The temperature dependence of the effective magnetic field on ^{57}Fe nuclei for sample 5 was used to determine the Néel temperature which was found to be 265 ± 10 K. The latter is in a good agreement with the data of Ref. (*10*).

Summary of Mössbauer Spectroscopy Data

Tracer charge state. In all samples Fe ions are in the 3+ state (isomer shifts δ^{Fe} have been found to range from 0.32 to 0.4 mm/sec). For Co_3O_4 this result is in agreement with Murray and Linnett (*13*) and Smith *et al.* (*18*). However, for the CoO matrix Fe^{3+} as well as Fe^{2+} ions were observed (*10, 11, 19, 20*) and the supposition was put forward that Fe^{3+} can be stabilized only by nearest-neighbor anion vacancies. Analysis of the synthesis conditions revealed that Fe^{2+} ions were detected only for samples prepared in conditions of low oxygen activity, e.g., by oxidation of Co–Fe alloy with CO_2 or by vacuum decomposition of basic carbonate. In our work the initial sample 1 was prepared in more oxidizing conditions and its subsequent treatment was carried out in a range of temperatures and oxygen partial pressures excluding the reduction of Fe^{3+} to Fe^{2+}.

Coordination. For all samples investigated, Fe^{3+} ions are in octahedral coordination, which agrees with Okand and Mullen (*10*) and Smith *et al.* (*18*). For the CoO phase with an NaCl structure, where only octahedral interstices are filled, such a state of the Fe ions is the most probable from the thermodynamic point of view. However, for

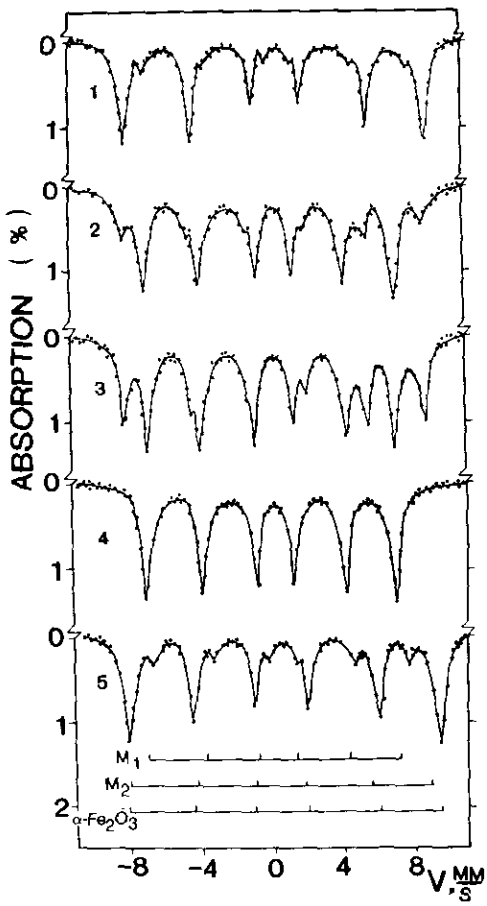

FIG. 3. Mössbauer spectra of the samples at 4.2 K. The curve designation is the same as in Fig. 2.

TABLE II

MÖSSBAUER PARAMETERS OF THE SAMPLES[a]

Sample number, phase	Temperature of measurements, K	Lines	δ^{Fe}	Quad. shift ε	Quad. split Δ	Peak width	H_{eff} ±3 kOe	Relative intensity of lines, ±10%
				±0.04 mm/sec				
1. α-Fe_2O_3 + $Co_xFe_{3-x}O_4$	298	M_0	0.36	−0.12		0.46	512	63
		D	0.32		0.58	0.52	—	37
	77	M_0	0.44	−0.11		0.39	527	60
		D	0.37		0.68	0.54	—	40
	4.2	M_0	0.46	−0.08		0.5	530	60
		M_1	0.65	−0.2		0.69	442	40
2. α-Fe_2O_3 + $Co_xFe_{3-x}O_4$	298	D	0.33		0.58	0.52	—	92
		M_0	0.34	−0.12		0.49	500	8
	77	D	0.37		0.68	0.54	—	89
		M_0	0.44	−0.11		0.52	516	11
	4.2	M_1	0.46	0.0		0.85	456	89
		M_0	0.44	−0.11		0.90	520	11
3. $Co_xFe_{1-x}O$ + $Co_xFe_{3-x}O$	298	D	0.32		0.57	0.51	—	100
		D	0.35		0.60	0.53	—	60
	77	M_2	0.47	−0.03		0.51	539	40
		M_1	0.41	−0.13		0.8	440	60
	4.2	M_2	0.52	−0.10		0.85	541	40
4. $Co_xFe_{3-x}O_4$	298	D	0.32		0.58	0.51	—	100
	77	D	0.38		0.54	0.40	—	100
	4.2	M_1	0.39	−0.14		0.85	443	100
5. $Co_xFe_{1-x}O$ + $Co_xFe_{3-x}O_4$	298	D	0.32		0.58	0.40	—	15
		S	0.4	0.0		0.51	—	85
	77	M_2	0.42	−0.02		0.65	542	100
		M_1	0.39	−0.15		0.77	441	20
	4.2	M_2	0.54	−0.01		0.75	545	80

[a] See footnote 1 in text.

the $Co_xFe_{3-x}O_4$ spinel structure, where Fe ions can be situated in tetrahedral (A) as well as octahedral (B) positions, the fraction of B sites occupied depends upon the iron content. Thus, for $0 < x < 2.5$, Fe^{3+} ions are distributed among the A and B positions. The increase of x leads to the decrease of the Fe_A^{3+} population, and at $x > 2.28$ the Fe^{3+} ions occupy only B sites (*13*, *18*). Therefore, in our case the localization of the Mössbauer tracer only in B position could be explained by its low concentration.

As follows from Table II, the room temperature spectrum of sample 5 was interpreted in terms of a singlet (CoO phase) and a doublet (Co_3O_4 phase) assigned in both cases to octahedrally coordinated Fe^{3+} ions. According to Murray and Linnett (*13*) and Tricher *et al.* (*14*), this difference indicates a substantially greater degree of distortion of oxygen octahedra in the spinel structure, namely, trigonal distortion in a ⟨111⟩ direction. At liquid helium temperature, the values of quadrupole shift ε for sextets M_1 and M_2 also differ considerably (−0.15 and −0.01 mm/sec, respectively), though due to the θ dependence an increased ε does not necessarily imply a larger Δ and vice versa. Thus, for sample 2 at 298 K Δ is large but for sextet M_1 at 4.2 K the quadrupole splitting is not visible due to a special relationship between the direction of the magnetic field

(along [100] axis) and the axis of distortion on the octahedral sites, i.e. angle $\theta = 54.7°$ or $\theta = 125.3°$. This feature is typical for many spinel ferrites including $Co_xFe_{3-x}O_4$ with $x < 2.00$ (*13*).

Effective Debye temperatures Θ_D were calculated using the temperature dependence of the recoilless fraction in Debye approximation (*21*). These values for α-Fe_2O_3 (sample 1), $Co_xFe_{3-x}O_4$ (sample 4), and $Co_xFe_{1-x}O_4$ (sample 5) are equal to 316 ± 20 K, 272 ± 15 K, and 236± 20 K, respectively. According to the Debye model, the force constant K could be estimated from Θ_D of crystals from the relation $K = mk^2\Theta_D^2/4h^2$, where m is the mass of the Fe atom, and k, the Boltzmann constant. For the compounds under investigation K was estimated to be equal to 0.86×10^5, 0.64×10^5, and 0.48×10^5 dyn/cm, respectively. In first approximation f' and its temperature dependence are determined by the rigidity of Fe atom bonding in a crystal lattice, i.e., by the number of bonds and their length. For Co_3O_4 the *Me*–O distance in octahedra is equal to 1.89 Å; for CoO the *Me*–O distance is equal to 2.13 Å. Therefore, the difference of the octahedrons' sizes is reflected in such parameters as θ_D, f', and f' (T).

The localization of α-Fe_2O_3 clusters. The f' value obtained for α-Fe_2O_3 clusters (0.6 ± 0.05) is somewhat higher than the earlier determined value for a fairly perfect sample of α-Fe_2O_3 prepared by calcination of α-FeOOH at 1273 K ($f' = 0.55 \pm 0.05$) (*22*). According to Suzdalev (*23*), the variation of the α-Fe_2O_3 particle dimensions from 1 μm to 30 Å causes only the decrease of f'. Therefore, the dynamic behavior of α-Fe_2O_3 inclusions could be appreciated only in the case when they are embedded in a Co_3O_4 matrix possessing its own dynamic properties.

3. Magnetic Measurements

To study the magnetic properties of the samples, a procedure usually utilized for the investigation of spin glasses was employed.

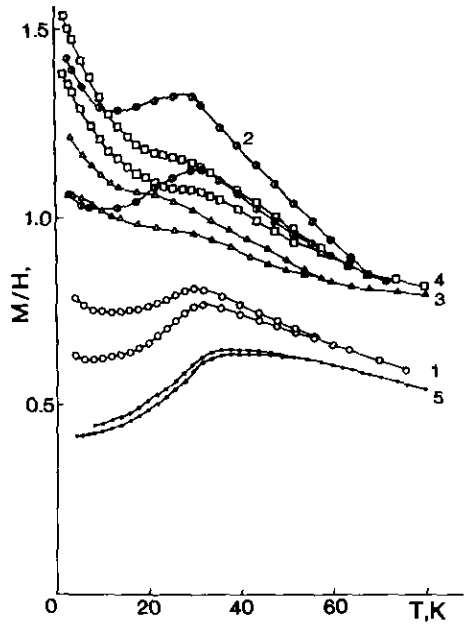

FIG. 4. The temperature dependence of the magnetic susceptibility of the samples investigated. (1–4) The same samples as in Tables I and II; (5)-pure Co_3O_4 calcined at 973 K.

In our case it enabled us to detect the processes of "freezing" (blocking) of magnetic clusters in the samples. The main results are given in Fig. 4. In the course of first heating of the sample isothermal susceptibility ($\chi_{ZFC}(T) = M_{ZFC}(T)/H$, where ZFC = zero field cooled) was measured. After cooling of the sample heated in magnetic field its thermostatic susceptibility ($\chi_{FC}(T)$, where FC = field cooled) was determined.

For pure Co_3O_4 (sample 6) behavior typical for antiferromagnetic susceptibility was observed: the susceptibility maximum is at ca. 40 K and then it decreases monotonically as temperature declines. The Neel temperature T_N determined by the maximum $d\chi/dT$ is ca. 31 K. For this sample an insignificant difference between the χ_{FC} and χ_{ZFC} is observed. It may be caused by the domain structure of the Co_3O_4 particles.

The addition of iron into cobalt oxides led to a variation of the samples' magnetic properties. For sample 1, which contains iron mainly in the form of α-Fe_2O_3 clusters

(vide supra), an increase of susceptibility due to a contribution from hematite was observed. The temperature dependence of susceptibility was changed only slightly except for an increase of the difference between the FC and ZFC branches. The latter could be explained by blocking of the α-Fe_2O_3 clusters and/or by an influence of the clusters on the domain structure of Co_3O_4.

For sample 2 a considerable variation of the magnetic properties as compared with those of pure Co_3O_4 and/or sample 1 was observed. It is manifested in the growth of susceptibility at low temperatures and in the appearance of significant hysteresis of susceptibility noticeable even at high temperatures, $T \gg T_N$. A low temperature growth of susceptibility indicates the presence of free magnetic moments of Fe ions and/or small clusters of α-Fe_2O_3 not participating in antiferromagnetic ordering. Small hematite clusters appeared to be the source of susceptibility hysteresis by the Néel mechanism of superparamagnetic particle blocking.

The temperature of blocking is a function of the magnetic cluster dimension. Since for samples 3 and 4 annealing at enhanced temperatures leads to the increase of low temperature susceptibility caused by free magnetic moments, it could be concluded that a decrease of cluster sizes takes place. Due to this phenomenon, for samples 3 and 4 the maximum of susceptibility is not observed, while the antiferromagnetic transition is manifested only as a bend on the $\chi(T)$ curve.

Discussion

Tracer Redistribution

The system investigated could serve as a model for studying the processes of ferrite formation and modification of the defect structure of oxides by microimpurities (*24*). In the course of solution evaporation numerous small nuclei were formed. The subsequent calcination at 673 K led to the sintering of the primary particles of Co_3O_4. However, there are Fe-enriched layers on the sintering surfaces; therefore, spinel structure becomes distorted and the joining of the particles cannot proceed coherently. This explains the formation of stacking faults and microinclusions of α-Fe_2O_3. A lesser part of iron was captured into the bulk of Co_3O_4 as isolated Fe^{3+} ions.

The increase of the calcination temperature up to 1073 K substantially accelerated the diffusion processes leading to the dissolution of α-Fe_2O_3 inclusions and to the increase of iron concentration in the spinel matrix. After calcination at 1273 K with subsequent annealing at 1073 K for the recovery of phase composition a fairly uniform distribution of iron in the Co_3O_4 matrix was attained. In the process of the tracer migration, a considerable gradient of iron throughout the spinel matrix inevitably occurs. A substantial nonequilibrium in the Fe distribution among the spinel positions could also be supposed. Indeed, sample 2 has a higher value of magnetic susceptibility as compared with sample 1 and the highest value of H_{eff} for M_1 sextet that could indicate exchange or superexchange interactions between the Fe ions in the Co_3O_4 lattice within the "diffusion" zone. Since the interaction between the ions in octahedra (B–B exchange) is usually very weak (*24*), for this phenomenon to be observed part of the Fe ions must be located in positions usually vacant in the spinel structure.

The Features of the Defect Structure of Cobalt Oxides

The two-phase CoO–Co_3O_4 system (sample 3) has a well-developed dislocation network. It is known that line width is sensitive to the presence of extended defects including dislocations (*25*, *26*). Indeed, Mössbauer parameters for the CoO phase in this sample substantially differ from those typical for a well-annealed CoO specimen (sample 5): for sextet M_2 quadrupole splitting ε and line width $\Gamma_{1,6}$ are enhanced. As is seen from the value of an increased line width for doublet D at 77 K, the Co_3O_4 phase in sample 3 is also not ideal. Therefore, in the two-phase

system obtained by oxidation of CoO both phases are disordered.

High-temperature phase of CoO was also found not to be ideal. The presence of Co_3O_4 clusters in sample 5 is evident from the data given in Table II. These results are in agreement with the literature data (*8*, *9*) where the microheterogeneity of CoO was supposed to accompany an excess of oxygen in nonstoichiometric samples.

An ordered array of extended defects for sample 5 could possibly be associated with preferential location of Fe^{3+} in some planes of CoO matrix. This could create either stacking faults and twins or spinel interlayers enriched by oxygen.

The isomer shift δ is known to decrease with diminishing of the electron density on ^{57}Fe nuclei. In our case all samples contain Fe^{3+} only. However, some variation of the isomer shift could be expected due to the variation of environment caused by a change of the oxide matrix stoichiometry. Thus, for sample 1 as compared with sample 4, the isomer shift δ for M_1 sextet at 4.2 K is enhanced. The observed change of isomer shift in nonstoichiometric Co_3O_{4+x} can be explained by the generation of cation vacancies having negative effective charge. Such charge should lead to a relative increase of electron density on the neighboring ^{57}Fe nuclei and to increase of δ. This conclusion is favored also by the largest value of ε for this low-temperature phase indicating a distortion of the spinel structure. Therefore, the most probable model for the nonstoichiometric Co_3O_{4+x} is the one in which at least a part of cation vacancies is situated in octahedra. It favors the preferential localization of Fe ions in these positions in low temperature samples. It is not clear from our results whether these vacancies are located in the surface layer or in the bulk of the particles.

Acknowledgments

We are thankful to Dr. G. N. Kryukova for providing the TEM results and Dr. Yu. T. Pavlukhin for helpful discussions.

References

1. YU. D. TRETYAKOV, "Chemistry of Non-stoichiometric Oxides," Moscow State University, 1974.
2. I. D. BELOVA, YU. E. ROGINSKAYA, AND YU. I. VENEVTSEV, *Zh. Neorg. Khim.* **28,** 3009 (1983). [Russian]
3. YA. M. KOLOTYRKIN, I. D. BELOVA, YU. E. ROGINSKAYA, V. B. KOZHEVNIKOV, D. S. ZAKHAR'IN, AND YU. N. VENEVTSEV, *Mater. Chem. Phys.* **11,** 29 (1984).
4. I. S. KOTOUSOVA AND S. M. POLYAKOV, *Kristallografiya* **17,** 661 (1972). [Russian]
5. S. ANGELOV, E. ZHECHEVA, AND D. MEHANDJIEV, *Izv. Otd. Khim. Nauki Bulg. Akad. Nauk.* **12,** 641 (1979).
6. I. D. BELOVA, V. V. SHALAGINOV, B. SH. GALYAMOV, YU. E. ROGINSKAYA, AND D. M. SHUB, *Zh. Neorg. Khim.* **23,** 286 (1978). [Russian]
7. S. ANGELOV, E. ZHECHEVA, AND D. MEHANDJIEV, *Izv. Otd. Khim. Nauki Bulg. Akad. Nauk.* **13,** 369 (1980).
8. C. R. A. CATLOW, W. C. MACKRODT, M. G. NORGETT, AND A. M. STONEHAM, *Philos. Mag. A* **40,** 161 (1979).
9. J. NOWOTNY, M. SLOMA, AND W. WEPPNER, *In* "Non-stoichiometric Compounds: Surfaces, Grain Boundaries and Structural Defects" (J. Nowotny and W. Weppner, Eds.), pp. 265–278, Kluwer Academic, Dordrecht/Boston/London (1989).
10. H. N. OKAND AND J. S. MULLEN, *Phys. Rev. B* **168,** 550 (1968).
11. F. S. NASREDINOV AND A. V. ERMOLAEV, *Phys. Status Solidi* **74,** 631 (1982).
12. N. YAMAMOTO, *J. Phys. Soc. Jpn.* **24,** 23 (1968).
13. P. J. MURRAY AND J. W. LINNETT, *J. Phys. Chem. Solids* **37,** 619 (1976).
14. M. J. TRICHER, P. P. VAISHNAVA, AND D. A. WHAN, *Appl. Catal.* **3,** 283 (1982).
15. "Gmelin Handbuch der Anorg. Chem.," 8 Aufl., Kobalt, Teil A, Verlag Chemie, GmbH, Berlin (1932).
16. YU. F. BABIKOVA, N. C. KOLPAKOV, K. E. NILIN, AND I. I. SHTAN, *Prib. Tekh. Eksp.* **4,** 44 (1983).
17. W. KÜNDIG, H. BÖMMEL, G. CONSTABARIS, AND R. LINDQUIST, *Phys. Rev.* **142,** 327 (1966).
18. P. A. SMITH, C. D. SPENCER, AND R. P. STILLWELL, *J. Phys. Chem. Solids* **39,** 107 (1978).
19. W. KÜNDIG, M. KOBELT, H. APPEL, G. CONSTABARIS, AND R. LINDQUIST, *J. Phys. Chem. Solids* **30,** 819 (1969).
20. G. K. WERTHEIM, *Phys. Rev. B* **124,** 764 (1961).
21. K. S. SINGWI AND A. SJÖLANDER, *Phys. Rev.* **120,** 1093 (1960).
22. V. I. KUZNETSOV, V. A. SADYKOV, M. T. PROTASOVA, AND G. S. LITVAK, *Izv. Sib. Otd. Akad. Nauk SSSR Ser. Khim. Nauki* **2,** 112 (1990). [Russian]

23. I. P. SUZDALEV, "Dynamic Effects in Resonance Spectroscopy," p. 55, Atomizdat, Moscow (1979).
24. E. B. LEVIN, YU. D. TRETYAKOV, AND L. M. LETYUK, "Physico-chemical Basis of Synthesis, Properties and Application of Ferrites," Metallurgia, Moscow (1979).
25. YU. T. PAVLUKHIN, YA. YA. MEDIKOV, AND V. V. BOLDYREV, *Izv. Sib. Otd. Akad. Nauk SSSR* **5,** 46 (1983).
26. YU. T. PAVLUKHIN, YA. YA. MEDIKOV, AND V. V. BOLDYREV, *J. Solid State Chem.* **53,** 115 (1983).